

Genetic study of gutter-shaped root (GSR) in AKXL RI mouse strains using QTL analysis

Itaru Tashima, Koichiro Arita and Yoshinobu Asada

Department of Pediatric Dentistry, Tsurumi University School of Dental Medicine, Yokohama, Japan

(Received 13 October 2009 and accepted 10 February 2010)

Abstract: In this study, quantitative trait locus (QTL) analysis was used to identify candidate chromosomes and for detecting the regions that include the gene or genes causing gutter-shaped root (GSR) in AKXL recombinant inbred mouse strains. One potential QTL was detected on chromosome 5 within a region of 13.0 cM, where the likelihood ratio statistic (LRS) score was higher than a suggestive level. This indicates that one of the candidate genes causing mouse GSR may be located in this region. (*J Oral Sci* 52, 213-220, 2010)

Keywords: AKXL RI mice; Gutter-shaped root; QTL analysis; dental root fusion rate.

Introduction

Abnormal root morphogenesis in human mandibular second or third molars occurs frequently. One of these abnormalities is known as gutter-shaped root (GSR), in which the root appears to be fused. It is well known that root canal treatment of teeth with fused roots is challenging and has a worse prognosis than that for a normal root (1). Teeth with GSR are also likely to have a poor prognosis when affected by periodontal disease. The morphological features of GSR have been reported by many investigators (2,3).

It has been reported that C57L/J mice have fused roots similar to GSR on their lower second molars, and they are therefore one of the most useful animal models for studying

the cause of GSR formation (4). Previous research has suggested that an autosomal-dominant inheritance pattern affects the development of mouse GSR, and that several genes may be involved (5,6). However, the major gene responsible has not yet been specified. Arita et al. recently reported a new method for measuring mouse GSR as a quantitative trait using micro-CT imaging (7). Therefore, quantitative trait locus (QTL) analysis has become feasible for determining the candidate genes responsible for GSR formation. QTL analysis has been used successfully for identifying chromosomal regions that exert quantitative effects due to poly genes, determining traits such as body weight and susceptibility to alcoholism (8,9).

Recombinant inbred (RI) strains of mice are useful for the study of complex traits such as body weight (10,11). RI mouse strains are derived from systematic inbreeding of randomly selected pairs of the F2 generation of a cross between two different inbred strains. The AKXL RI strain is an existing strain derived from the mouse AKR/J and C57L/J progenitor strains, both of which have been well characterized, and show differences in a variety of phenotypes, such as cholesterol gallstone formation (12,13). AKR/J mice do not have abnormal tooth roots. Therefore, it is thought that different strains of AKXL RI mice may have a variety of root shapes in the lower second molar. In this study, we focused on identifying the chromosomal regions involved in mouse GSR formation. Here we report genetic analysis of GSR formation in AKXL RI strains using QTL analysis.

Materials and Methods

Experiment 1

Mice

A total of 44 mice obtained from paternal strains (2 males and 2 females for each of C57L/J, AKR/J, BALB/cAnNCrIcrIj, C57BL/6J, C3H/HeJ, and DBA/2J) and F1

Correspondence to Dr. Itaru Tashima, Department of Pediatric Dentistry, Tsurumi University School of Dental Medicine, 2-1-3 Tsurumi, Tsurumi-ku, Yokohama 230-8501, Japan
Tel: +81-45-581-1001
Fax: +81-45-583-9599
E-mail: Itaru-tashima@tsurumi-u.ac.jp.

mice (2 males and 2 females for each of C57L/J×AKR/J, C57L/J×BALB/cAnNCrICrIj, C57L/J×C57BL/6J, C57L/J×C3H/HeJ, and C57L/J×DBA/2J) were used. Parental strains were obtained from the Jackson Laboratory (Bar Harbor, ME, USA) and Japan Charles River Company (Yokohama, Japan). All mice were raised under conventional conditions: $25 \pm 2^\circ\text{C}$, $55 \pm 5\%$ humidity, and 12L/12D light. The mice were fed a pellet diet (MR Breeder, Nihon Nohsan Company, Yokohama, Japan) and tap water *ad libitum*. All experimental protocols concerning animal handling were reviewed and approved by the Institutional Animal Care Committee of Tsurumi University School of Dental Medicine.

Measurement of mouse GSR

At the age of 35 days, the mice were anesthetized with ether and euthanized. The heads were soaked in 1% KOH at 42°C for 48 h, the mandibles were removed and washed with water, and the soft tissue was removed. The mandible bones were then washed with water and dried. The lower second molars (M2) were then extracted. The dental root fusion rate (DRFR) was calculated (Fig. 1) according to Arita's method (7). The DRFR data were expressed as scores for individual F1 groups or as mean \pm SD, as appropriate.

Experiment 2

Mice

A total of 66 mice obtained from parental strains (3 males and 3 females for each of C57L/J and AKR/J) and AKXL RI strains (3 males and 3 females for each of the 9 RI strains) were used. Parental-strain mice were obtained from the Jackson Laboratory, and RI mice from the RIKEN BioResource Center (Tsukuba, Japan).

Measurement of mouse GSR

The mice were raised under the same conditions, and the DRFR was calculated in the same way, as in Experiment 1.

QTL analysis

The strain distribution pattern (SDP) of polymorphic markers was used in the QTL analysis (Mouse Genome Informatics <http://www.informatics.jax.org/>). We used a total of 201 markers on autosomal chromosomes for interval mapping (Table 1). Genomic interval mapping was performed using Map Manager QTX b20 software to identify the chromosomal location of quantitative trait loci (14). The criteria for statistical significance in the mapping were determined by a permutation test, and then we obtained logarithm of odds (LOD) scores (15). Three statistical significance thresholds were estimated with a permutation test (1,000 iterations) for the empirical probability of the relationship between the putative locus of the gene and the value of the trait: $P < 0.67$ for a suggestive correlation only, $P < 0.05$ for a statistically significant correlation, and $P < 0.001$ for a highly significant correlation (16).

Results

Experiment 1

DRFRs were calculated on the M2 in F1 mice and paternal strains (Fig. 2). In F1 mice, the highest DRFR was seen in C57L/J×AKR/J (91.5%), followed in decreasing order by C57L/J×C57BL/6J (50.0%), C57L/J×C3H/HeJ (35.4%), C57L/J×DBA/2J (26.1%) and C57L/J×BALB/cAnNCrICrIj, (18.0%). DRFRs of paternal strains were as follows: C57L/J (100%), AKR/J (24.0%), C57BL/6J (25.6%), C3H/HeJ (27.2%), DBA/2J (20.9%), and

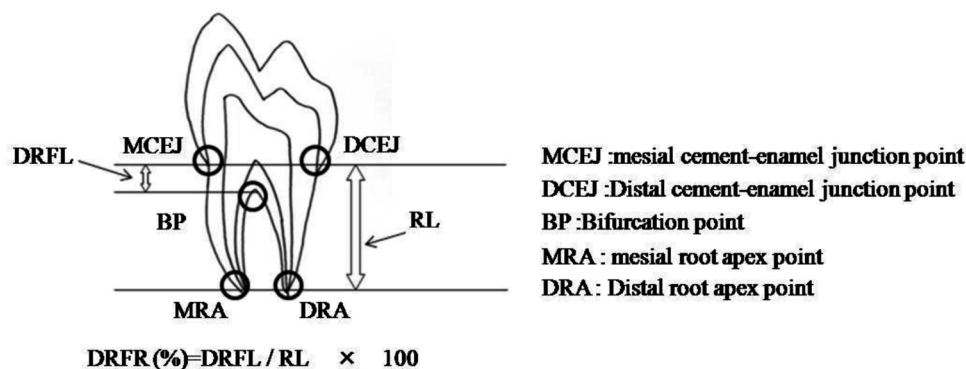


Fig. 1 Measurement of root length (RL) and dental root fusion length (DRFL), and calculation of dental root fusion rate (DRFR). Following the methods of Arita et al. (7), the tooth was scanned by micro-CT, and the scanning data were reconstructed and drawn on a PC display to allow calculation.

Table 1-1 Polymorphic markers list

Chromosome	Maker	cM position	Chromosome	Maker	cM position		
Chr1	D1Rp2	10.00	Chr3	D3Pas1	22.70		
	Lmyc2	15.40		D3Mit6	23.30		
	Gas10	25.90		D3Mit7	26.40		
	Nppc	54.00		Xmmv47	30.20		
	Mlph	59.00		D3Mit51	362.00		
	Mpmv6	69.10		D3Mit40	39.70		
	Mpmv16	69.90		Amy2	50.00		
	Serpinc1	84.60		Pmv26	75.00		
	Fcgr3	92.30		D3Mit19	87.60		
	Xmv41	92.60		Chr4	Xmmv62	syntenic	
	Spna1	95.40			D4Mit2	6.50	
	Mtv7	96.00			Ras12-7	21.30	
	D1Bir2	101.50			Mup1	27.80	
	Pmv21	106.00			Tyrp1	38.00	
	Chr2	Serping1			syntenic	Ipp	51.40
		Tnfaip6			syntenic	Pmv19	52.70
		D2Mit64			18.00	Mycl1	55.00
D2Mit7		28.00	Pou3f1		56.10		
Pmv7		33.00	Alpl		70.20		
D2Mit56		41.00	D4Ty1		73.00		
Lith1		syntenic	Dvl1		82.00		
D2Mit11		41.80	Chr5		D5Bir2	13.00	
D2Mit35		45.00			Plk-ps1	18.00	
D2Mit14a		49.60			D5Bir3	24.00	
Mpmv14		62.00			Qdpr	30.00	
Actc1		64.00			Xmv38	32.00	
D2Mit109		81.70		Pmv11	43.00		
Emv13		87.50		Fla	67.00		
Svs5		94.00		Phkg1	72.00		
Pmv33		98.00		Epo	78.00		
Chr3		Car2		10.50	Chr6	D6Mit86	0.50
	D3Mit46	13.80		Mtv23		16.00	
	Mpmv20	13.80		Fabp1		30.00	
	Evi1	14.40		D6Mit21		35.15	
	D3Mit21	19.20		D6Mit40		37.00	

BALB/cAnNCrIcrlj (18.4%).

Experiment 2

Phenotype analysis

DRFRs on the M2 in RI mice ranged from 0 to 100% (Fig. 3). The highest DRFR was seen in C57L/J (100%) and AKXL6 (100%), followed in decreasing order by AKXL16 (90.0%), AKXL37 (86.0%), AKXL17 (62.2%), AKXL38 (53.6%), AKXL21 (38.9%), AKXL14 (29.3%), AKXL13 (27.0%), AKR/J (24.1%) and AKXL9 (20.1%). DRFR was expressed as a continuous trait distribution pattern in RI mice.

QTL analysis

The results of QTL analysis for GSR are shown in Fig.

4. One suggestive QTL was detected. Around the marker D5Bir2, a region 13.0 cM from the centromere on chromosome 5, the LOD score was higher than the suggestive level. Significant or suggestive QTLs were not obtained for any other chromosomes.

Discussion

Experiment 1

It is known that GSR is characterized by several genetic factors on autosomal chromosomes (5,6). In this study, the DRFRs of F1 mice were calculated for a variety of phenotypes, and our findings were consistent with previous studies. F1 mice derived from breeding of C57L/J and AKR/J strains had the highest average DRFR (91.5%) in this study. High penetrance was observed in the F1

Table 1-2

Chromosome	Maker	cM position	Chromosome	Maker	cM position
Chr6	Il5ra	46.00	Chr10	D10Mit75	2.00
	Rho	51.50		D10Nds1	6.00
	Es12	61.50		D10Mit106	173.00
Chr7	Prh1	63.60	D10Mit130	31.50	
	Emv11	3.00	D10Mit175	41.80	
	Pmv29	5.00	D10Mit42	44.00	
	Upk1a	10.00	D10Mit180	64.00	
	Cebpa	12.00	Chr11	Pmv22	8.00
	Fau-ps3	18.90		Egfr	9.00
	Gas2	26.80		Hba	16.00
	Fes	39.00		Emv14	37.00
	Hbb	50.00		D11Nds1	43.80
	Odc-rs7	51.50		Xmv42	53.00
	Rasl4	55.00		Cnp	60.00
	Itga1	60.00		D11Kyo1	64.00
	Il4ra	62.00		Es3	74.00
	Th	69.20		Galk1	78.00
Fgf3	72.40	Tk1	78.00		
Chr8	D8Mit23	8.00	Chr12	Mtv30	1.00
	D8Mit177	30.00		Odc1	6.00
	D8Mit25	32.00		D12Nyu20	7.00
	D8Mit9	33.50		D12Nyu19	8.00
	D8Mit45	40.00		D12Nyu2	9.00
	D8Mit42	71.00		Ahr	18.00
Chr9	Xmv16	24.00		Ltw2	18.00
	Cd3d	26.00		Ly18	18.00
	Cyp1a2	31.00		Lamb1-1	20.00
	Gsta1	43.00		D12Nyu5	22.00
	Pgm3	48.00		D12Nyu1	23.00
	Rasl2-2	54.00		D12Nyu15	23.00
	D9Kyo1	57.00	Pmv3	23.00	
	Ltw3	60.00	Mpmv11	30.00	
	Mst1r	60.00	D12Mit4	34.00	
	Ryk	61.00	Tshr	37.00	
Cck	71.00	Pmv27	48.00		

(C57L/J×AKR/J) mice. Hence, it is suggested that the AKR/J mouse strain is the most useful for QTL analysis when hereditary inbreeding is conducted using F2, N2 or RI strains. Therefore, we selected AKXL strains for QTL analysis in this study.

Experiment 2

According to the distribution pattern of the DRFR for each RI mouse, the phenotype showed continuous and quantitative genetic traits (Fig. 3). Our findings are consistent with previous studies suggesting that GSR is characterized by several genetic factors on the autosomal chromosomes.

Based on this result, we proceeded with QTL analysis, and detected one QTL that exceeded the suggestive

thresholds for the trait around D5Bir2 on chromosome 5 (Fig. 4). In a previous study, Shimizu reported that one of the candidate gene loci causing GSR formation in mice exists around D5Mit161 (70.0 cM) and D5Mit29, D5Mit321, D5Mit427 (the positions of these three markers lie within 72.0 cM) on chromosome 5 (5). Although the marker positions differed, the same chromosome was specified by two different experiments. These results provide strong support for the presence of a QTL on chromosome 5. In the same study, Shimizu reported that high score linkage was detected on chromosomes 8 and 17 (5). In our experiment, however, significant or suggestive QTLs were not obtained for any other chromosomes except chromosome 5. Relatively few AKXL strains were used in this experiment, because it was difficult to obtain more.

Table 1-3

Chromosome	Maker	cM position	Chromosome	Maker	cM position
Chr12	D12Mit7	50.00	Chr17	D17Leh66E	syntenic
	Serpina1	51.00		D1Tu5	3.82
	Ckb	55.00		D17Mit27	7.54
	D12H14S17	55.00		Rasl3	14.70
	D12N1	59.10		D17Tu10	16.88
Chr13	D13Mit1	1.00		D17H21S56	17.20
	D13Mit3	10.00		D17Mit21	18.64
	Pmv67	19.00		D17Rp11e	29.00
	Ly28	28.00		Rasl2-3	33.50
	D13Ty1	39.00		Hprt-ps1	47.60
	D13Mit107	48.00	D17Mit1	56.70	
	Lth1	54.00	Chr18	D18Mit19	2.00
	Pmv9	54.00		D18Mit110	4.00
	D13Rp4	67.00		D18Mit14	18.00
	D13Mit196	68.00		Cd74	32.00
Chr14	D13Mit78	75.00	D18Mit51	37.00	
	Mtv11	16.00	D18Mit9	42.00	
	Rnase1	18.50	D18Mit49	49.00	
	D14Mit214	19.00	D18Mit4	57.00	
	Carg1	19.50	Chr19	D19Mit59	0.50
Tera	19.50	Ms4a2		8.00	
Clu	28.00	D19Mit41		16.00	
Chr15	Xmv37	7.60		Rln1	21.00
	Tg	36.40		D19Mit40	25.00
	D15Mit1	46.30	D19Mit19	26.00	
Chr16	D16Mit9	4.00	D19Mit35	53.00	
	D6Mit12	27.60	D19Mit6	55.00	
	D16Ros1	31.50			
	D16Ros2	41.00			
	Xmv35	41.60			
	D16Mit47	43.00			
	Pmv14	45.60			
	Sod1	61.00			
D16Mit106	71.45				

Therefore, we consider that our results do not rule out the presence of a candidate on chromosomes 8 and 17.

The mouse genome database and map viewer (Mouse Genome Informatics; <http://www.informatics.jax.org/>) were searched for candidate genes corresponding to this region. Three candidate genes were found on chromosome 5; frizzled homolog 1 (*Fzd1*), solute carrier family 4 member 2 (*SLC4a2*), and sonic hedgehog (*SHH*). *Fzd1* is an antagonist of canonical Wnt/beta-catenin signaling (17), and this signaling pathway plays an important role during tooth development (18,19). *SLC4a2* is required for osteoclast differentiation and function (20). It is known that *SHH* and the *SHH* signaling pathway play an important role during tooth development (21,22). In particular, *SHH* signaling is required for tooth root morphogenesis (23,24), and it is reasonable to assume that minor differences in

this gene could produce different forms of the root.

In order to specify the candidate gene, a fine-mapping study with an F2 intercross or an N2 backcross will be required. The results of the present study and subsequent fine-mapping will help clarify the underlying mechanisms of dental root morphogenesis in humans, because mouse and human genes are highly syntenic, and the trait around D5Bir2 on chromosome 5 in mice is evolutionarily conserved on human chromosome 7.

Acknowledgments

The authors wish to thank Dr. K Ohno and Dr. Y Idaira, Department of Pediatric Dentistry, Tsurumi University School of Dental Medicine, for their helpful suggestions and advice.

This work was supported by a Grant-in-Aid for scientific

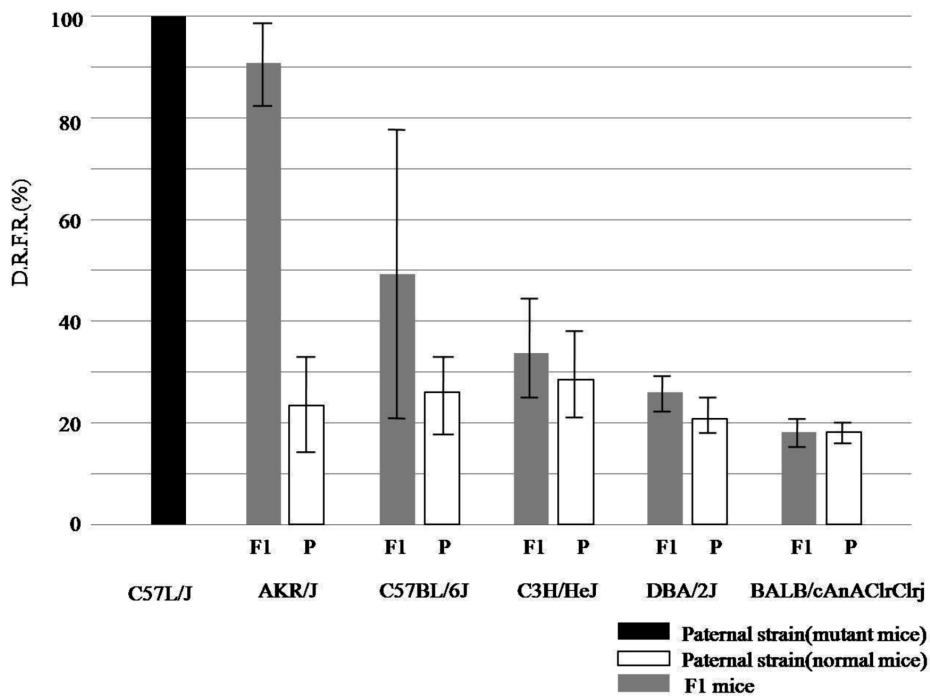


Fig. 2 DRFR of F1 mice and paternal strains. Vertical axis: percentage of DRFR; horizontal axis: individual F1 and each paternal strains. DRFRs were expressed as a percentage from 0% to 100%. The DRFR data were expressed as scores for individual groups or as mean \pm SD, as appropriate.

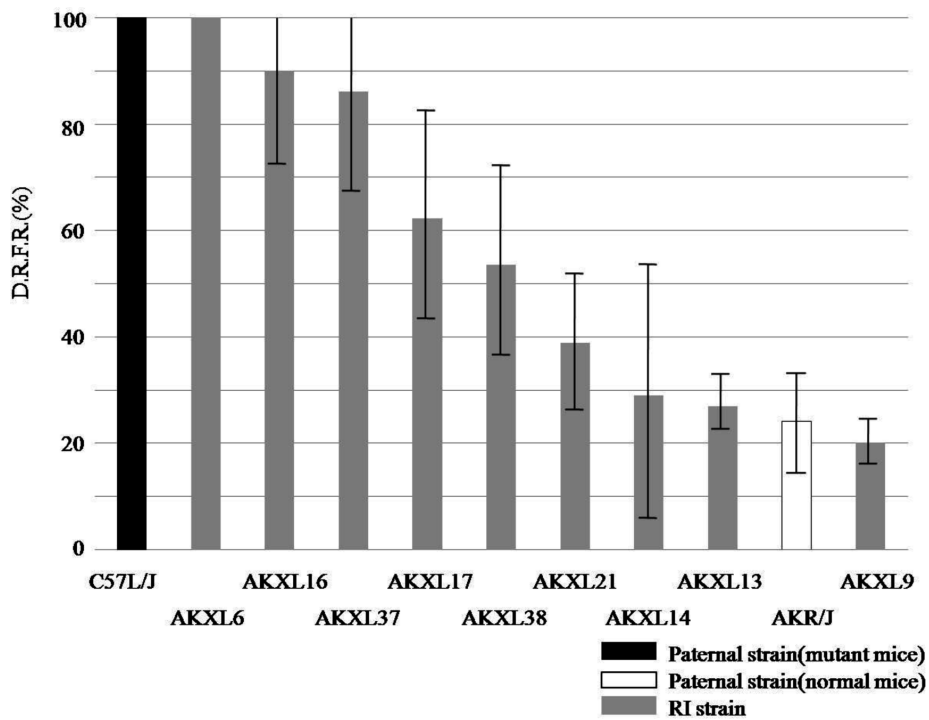


Fig. 3 Distribution pattern of C57L/J, AKR/J, and RI mice. Vertical axis: percentage of DRFR; horizontal axis: individual strains of C57L/J, AKR/J, and RI mice. DRFRs were expressed as a percentage from 0% to 100%. The DRFR data were expressed as scores for individual strain groups or as mean \pm SD, as appropriate.

Chromosome 5

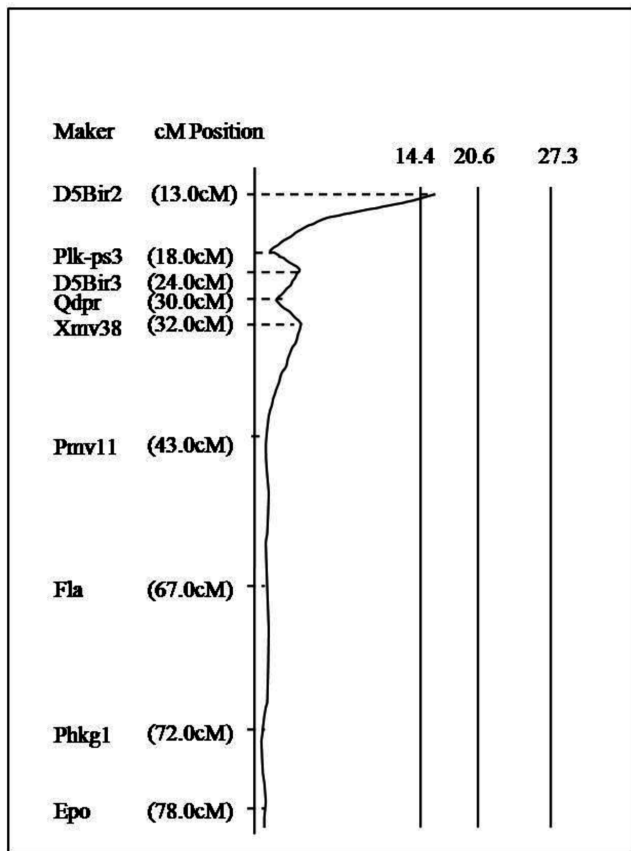


Fig. 4 Mapping of quantitative trait loci on chromosome 5. The vertical lines represented by the numerical values of 14.4, 20.6 and 27.3 indicate suggestive, significant and highly significant levels, respectively.

research (B) 19390534, 2007~2009.

References

1. Tsesis I, Steinbock N, Rosenberg E, Kaufman AY (2003) Endodontic treatment of developmental anomalies in posterior teeth: treatment of geminated/fused teeth – report of two cases. *Int Endod J* 36, 372-379.
2. Fukuya T (1976) A morphological study on gutter shaped root tooth. *Kyusyu Shika Gakkai Zasshi* 29, 557-576. (in Japanese)
3. Takahashi M, Asami Y, Kobayashi K (1991) Forming process of the gutter-shaped root of the human lower molar. *Shigaku* 79, 642-651. (in Japanese)
4. Asada Y (2001) Discovery and evaluation of the gutter shaped root (GSR) in inbred mice. *Shoni Shikagaku Zasshi* 33, 774-784. (in Japanese)
5. Shimizu T (1999) Mapping of a gene causing mouse gutter-shaped tooth root to chromosome 5. *Arch Oral Biol* 44, 917-924.
6. Matsune K (2000) Molecular genetic study of the gutter shaped root (GSR) on mouse chromosome 17. *J Oral Sci* 42, 21-26.
7. Arita K, Saito I, Arai Y (2006) Evaluation of mouse gutter shaped root(s) as a quantitative trait using micro-CT. *Pediatr Dent J* 16, 23-27.
8. Le Rouzic A, Alvarez-Castro JM, Carlborg O (2008) Dissection of the genetic architecture of body weight in chicken reveals the impact of epistasis on domestication traits. *Genetics* 179, 1591-1599.
9. Kozell L, Belknap JK, Hofstetter JR, Mayeda A, Buck KJ (2008) Mapping a locus for alcohol physical dependence and associated withdrawal to a 1.1 Mb interval of mouse chromosome 1 syntenic with human chromosome 1q23.2-23.3. *Genes Brain Behav* 7, 560-567.
10. Bennett B, Downing C, Carosone-Link P, Ponicsan H, Ruf C, Johnson TE (2007) Quantitative trait locus mapping for acute functional tolerance to ethanol in the LxS recombinant inbred panel. *Alcohol Clin Exp Res* 31, 200-208.
11. Anunciado RV, Ohno T, Mori M, Ishikawa A, Tanaka S, Horio F, Nishimura M, Namikawa T (2000) Distribution of body weight, blood insulin and lipid levels in the SMXA recombinant inbred strains and the QTL analysis. *Exp Anim* 49, 217-224.
12. Khanuja B, Cheah YC, Hunt M, Nishina PM, Wang DQ, Chen HW, Billheimer JT, Carey MC, Paigen B (1995) Lith1, a major gene affecting cholesterol gallstone formation among inbred strains of mice. *Proc Natl Acad Sci U S A* 92, 7729-7733.
13. Lammert F, Wang DQ, Paigen B, Carey MC (1999) Phenotypic characterization of Lith genes that determine susceptibility to cholesterol cholelithiasis in inbred mice: integrated activities of hepatic lipid regulatory enzymes. *J Lipid Res* 40, 2080-2090.
14. Manly KF, Cudmore RH Jr, Meer JM (2001) Map Manager QTX, cross-platform software for genetic mapping. *Mamm Genome* 12, 930-932.
15. Doerge RW, Churchill GA (1996) Permutation tests for multiple loci affecting a quantitative character. *Genetics* 142, 285-294.
16. Lander E, Kruglyak L (1995) Genetic dissection of complex traits: guidelines for interpreting and reporting linkage results. *Nat Genet* 11, 241-247.
17. Roman-Roman S, Shi DL, Stiot V, Haÿ E, Vayssière B, Garcia T, Baron R, Rawadi G (2004) Murine Frizzled-1 behaves as an antagonist of the canonical Wnt/beta-catenin signaling. *J Biol Chem* 279, 5725-

- 5733.
18. Järvinen E, Salazar-Ciudad I, Birchmeier W, Taketo MM, Jernvall J, Thesleff I (2006) Continuous tooth generation in mouse is induced by activated epithelial Wnt/beta-catenin signaling. *Proc Natl Acad Sci U S A* 103, 18627-18632.
 19. Chen J, Lan Y, Baek JA, Gao Y, Jiang R (2009) Wnt/beta-catenin signaling plays an essential role in activation of odontogenic mesenchyme during early tooth development. *Dev Biol* 334, 174-185.
 20. Wu J, Glimcher LH, Aliprantis AO (2008) HCO3-/Cl- anion exchanger SLC4A2 is required for proper osteoclast differentiation and function. *Proc Natl Acad Sci U S A* 105, 16934-16939.
 21. Gritli-Linde A, Bei M, Maas R, Zhang XM, Linde A, McMahon AP (2002) Shh signaling within the dental epithelium is necessary for cell proliferation, growth and polarization. *Development* 129, 5323-5337.
 22. Zhang L, Hua F, Yuan GH, Zhang YD, Chen Z (2008) Sonic hedgehog signaling is critical for cytodifferentiation and cusp formation in developing mouse molars. *J Mol Histol* 39, 87-94.
 23. Nakatomi M, Morita I, Eto K, Ota MS (2006) Sonic hedgehog signaling is important in tooth root development. *J Dent Res* 85, 427-431.
 24. Khan M, Seppala M, Zoupa M, Cobourne MT (2007) Hedgehog pathway gene expression during early development of the molar tooth root in the mouse. *Gene Expr Patterns* 7, 239-243.